

Photoluminescence from gas-suspended SiO_x nanoparticles synthesized by laser ablation

David B. Geohegan,^{a)} Alex A. Poretzky, Gerd Duscher, and Stephen J. Pennycook
Solid State Division, Oak Ridge National Laboratory, Oak Ridge, Tennessee 37831-6056

(Received 10 March 1998; accepted for publication 19 May 1998)

Time-resolved photoluminescence (PL) spectra are reported for gas-suspended 1–10 nm diameter SiO_x particles formed by laser ablation of Si into 1–10 Torr He and Ar. Three spectral bands (1.8, 2.5 and 3.2 eV) similar to PL from oxidized porous silicon were measured, but with a pronounced vibronic structure. Particle size and composition were determined with Z-contrast transmission electron microscopy imaging and high resolution electron energy loss spectroscopy linescans of individual nanoparticles. Maximized violet (3.2 eV) PL from the gas-suspended nanoparticles was correlated with an *ex situ* $\text{SiO}_{1.4}$ overall particle stoichiometry. Cryogenically-collected gas-suspended nanoparticles produced web-like-aggregate films exhibiting very weak PL. Standard anneals restored strong PL bands without vibronic structure, but otherwise in agreement with the PL measured from the gas-suspended nanoparticles. © 1998 American Institute of Physics.
[S0003-6951(98)02730-2]

Luminescent nanoparticles of 1–10 nm diameters are highly desirable optoelectronic materials since quantum confinement (QC) of electron-hole pairs can result in bright luminescence from new or previously forbidden optical transitions.¹ The size of the luminescent centers in porous silicon (*P-Si*) and nanocrystalline Si (*nc-Si*) was recently traced to sub-1.5-nm diameters (i.e., Si clusters of <30 atoms).²

Laser ablation is a versatile vaporization tool, and has recently been used to form photoluminescent films of *nc-Si* and silicon-rich silicon oxide (SRSO) nanoparticles in various modifications of the pulsed laser deposition technique.^{3–8} However, the temporal and spatial scales for nanoparticle formation in laser ablation plumes are just now becoming understood.^{5,9,10}

Here we report *in situ* time-resolved photoluminescence measurements of SiO_x nanoparticles as they form, oxidize, and transport following ablation of *c-Si* targets into 1 Torr Ar (99.9995%) or 10 Torr He (99.9999%). Gas-suspended nanoparticles were spatially and temporally located by gated-ICCD photography of Rayleigh-scattering (RS) and photoluminescence (PL) induced by a time-delayed XeCl laser pulse (308 nm, 4.0 eV, 25 ns FWHM).¹⁰

The dramatically different dynamics of SiO_x nanoparticle formation and transport were recently revealed with time-resolved imaging.¹⁰ Holey carbon-coated or bare copper transmission electron microscopy (TEM) grids were positioned on wire armatures in the chamber to collect the nanoparticles. PL and RS photography permitted direct imaging and control of the deposition process.¹⁰ The grids were exposed to room air for less than 2 min during loading into a VG HB501UX scanning transmission electron microscope (STEM) for Z-contrast imaging.

For *c-Si* ablation into 1 Torr Ar or 10 Torr He, spherical 5 nm diameter nanoparticles were collected (2 cm from the target) with other sizes ranging from 1 to 10 nm. For deposits collected after 1–10 laser shots, individual and small

groups of nanoparticles [as in Fig. 1(c)] were found. For deposits collected after hundreds of laser shots, groups of ~5 nm particles were also found in wire-like formations [Fig. 1(d)] or more often aggregates of up to 100–300 nm dimensions [Figs. 1(e) and 1(f)]. Under scanning electron microscopy (SEM) investigation, these aggregates interlinked to form a web-like microstructure very similar to those reported by El-Shall *et al.*⁴

Individual nanoparticles were examined for composition and nanostructure with high-resolution electron energy loss spectroscopy (HREELS, 0.27 nm spatial resolution, energy resolution ~0.8 eV). The intensity and energy loss near edge structure (ELNES) were examined at the Si–L absorption edge in Si (99 eV) and SiO_2 (102 eV), and at the O–K absorption edge to determine the nanoparticle composition. As shown in Fig. 1(a), particles were found with stoichiometries between nearly-pure Si to nearly-pure SiO_2 .

Compositional profiles of individual SiO_x nanoparticles were acquired by translating the STEM beam [as indicated in Fig. 1(c)] while ~100 ELNES spectra were recorded. These HREELS linescans showed [as in Fig. 1(b)] a uniform distribution of $\text{Si}^{(0)}$ bonding (as in pure silicon) and $\text{Si}^{(4+)}$ bond-

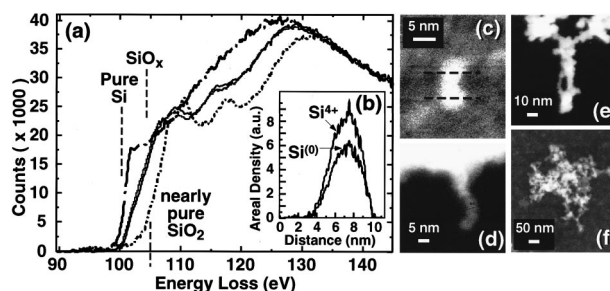


FIG. 1. High-resolution transmission EELS spectra of individual nanoparticles [collected on the grid in Fig. 2(a)], and imaged by Z-contrast TEM, show (a) a variation of stoichiometries ranging from pure silicon to nearly-pure SiO_2 . (b) Spatial distribution of pure-Si ($\text{Si}^{(0)}$) and pure- SiO_2 ($\text{Si}^{(4+)}$) silicon bonding within individual nanoparticles [shown in (c)] obtained from sets of ELNES spectra. Z-contrast TEM images showed 1–10 nm particles alone or (c) aggregated in pairs, suspended wire-like protrusions (d), three-dimensional networks (e), and network aggregates (f) of ~100–200 nm size.

^{a)}Electronic mail: odg@oml.gov

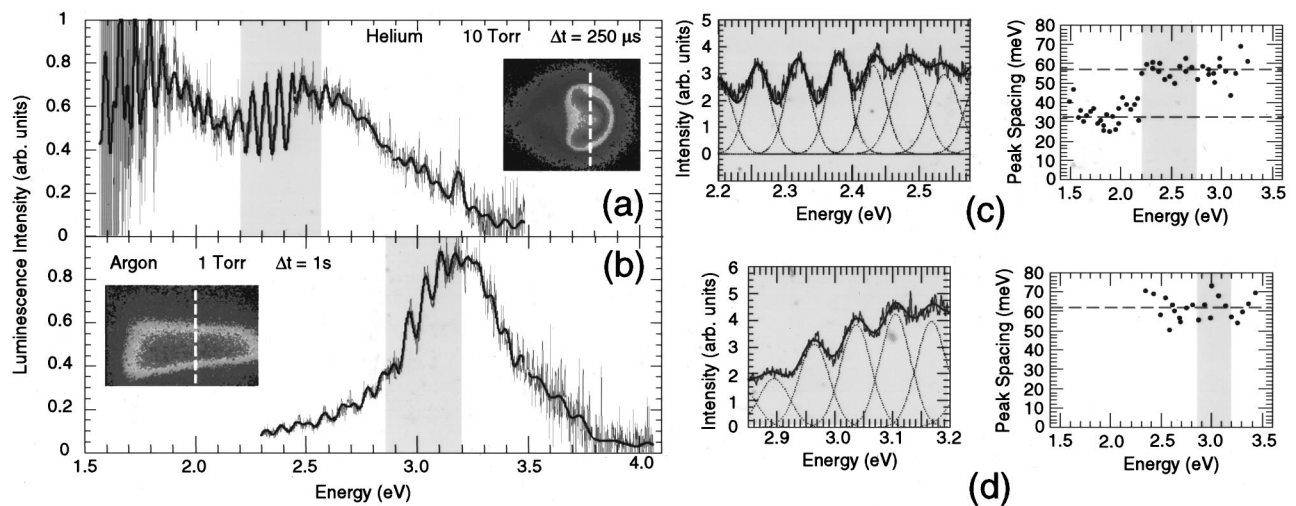


FIG. 2. Gated photoluminescence spectra from XeCl-laser-excited, gas-suspended nanoparticles 2 cm away from a laser-ablated Si target in (a) 10 Torr helium, $\Delta t = 250 \mu\text{s}$ after the ablation laser, and (b) 1 Torr argon, $\Delta t = 1 \text{ s}$. Ten-shot averaged spectra, 2.6 nm resolution, 3 μs gate (starting 150 ns after the XeCl excitation pulse). The shaded regions are replotted in (c) and (d), to show that the spectra can both be deconvoluted as a sum (shown by the blue curve) of Gaussian spectral bands. The spacing between adjacent band peaks is plotted vs peak PL energy. Single vibronic series fit the 3.2 and 2.5 eV bands (see text) while the 1.8 eV band in helium appeared to contain an additional vibronic series (an average interpeak spacing of $34 \pm 6 \text{ meV}$ is shown).

ing (as in pure SiO_2). The particles appear to be composed of a homogeneous mixture of pure and oxidized Si regions, which contrasts with surface-oxidized Si nanoparticles produced and analyzed in other studies.² Although the TEM resolution was sufficient to resolve lattice fringes from *c*-Si by Z-contrast imaging, repeated attempts were unsuccessful, indicating either amorphous silicon or *c*-Si regions in the sub-1 nm size range (i.e., clusters of *c*-Si < 25 atoms).

The *ex situ* stability of as-deposited nearly-pure silicon nanoparticles indicates that oxidation leading to the overall stoichiometry is accomplished in the gas phase. In argon, a weak flow was necessary to produce photoluminescence.¹⁰ No-flow or excessive Ar flow quenched the PL. In all cases where violet gas phase PL was observed, SRSO nanoparticles were collected. Introduction of oxygen-containing impurities (oxygen, water vapor) to condensing Si nanoparticles was controlled by increasing the Ar flow. The gas-phase violet PL was maximized by adjusting the flow rate of Ar (270 sccm) into the 50 ℓ chamber. This condition correlated with an overall *ex situ* $\text{SiO}_{1.4}$ stoichiometry.

PL spectra of gas-suspended nanoparticles are presented in Fig. 2 and Fig. 3(a). Three broad PL bands (centered at 1.8, 2.5, 3.2 eV) were found in varying proportions.¹⁰ For $\Delta t < 300 \mu\text{s}$ after ablation into 10 Torr He, the spectrum is composed of just two bands [at 1.8 and 2.5 eV, as in Fig. 2(a)], while at later times ($\Delta t > 300 \mu\text{s}$) a third band at 3.2 eV emerges to become the dominant emission [shown in Fig. 3(a)]. In 1 Torr Ar, the violet 3.2 eV band can be maximized as described above, as shown in Fig. 2(b) for $\Delta t = 1 \text{ s}$. In these experiments, all three bands shown in Figs. 2 and 3 had similar experimentally measured luminescence decay times of 1.8 μs (see Fig. 2 of Ref. 10).

The broad luminescence bands at 1.8, 2.5 and 3.2 eV are very similar to PL observed for oxidized *P*-Si and *nc*-Si.¹¹ While the calculated band gaps of sub-1.5-nm Si clusters extend from the blue to the ultraviolet (3–5 eV)¹² and direct transitions in *nc*-Si have been reported,¹³ the blue-green and violet bands are most often associated with fast oxidation of *P*-Si or *nc*-Si during production or post-processing

treatments.^{11,14–17} This is consistent with the evolution of the violet band during gas-phase oxidation in our experiments.

A pronounced oscillatory structure decorates each of the three PL bands. This structure was reproducible at different time delays with the most pronounced oscillations [Figs. 2(c), 2(d)] appearing on the low-energy sides of the bands. The entire spectrum could be deconvoluted as a sum of Gaussian line shapes. The spacing between neighboring peaks is plotted versus peak position in Figs. 2(c) and 2(d). For the 3.2 eV band in Fig. 2(b), the spacing is quite uniform ($62 \pm 6 \text{ meV}$). This roughly agrees with the spacing observed for the 2.5 eV band of Fig. 2(a) ($57 \pm 5 \text{ meV}$). The 1.8 eV band of Fig. 2(a) appeared to contain an additional vibronic series [an average interpeak spacing of $34 \pm 6 \text{ meV}$ is shown in Fig. 2(d)].

The apparent vibronic structure in Fig. 2 is suggestive of the phonon-assisted transitions (bulk TO and TA modes of *c*-Si at 57 and 18 meV) observed in resonantly-excited PL spectra of *P*-Si at low temperatures.¹⁸ However, only

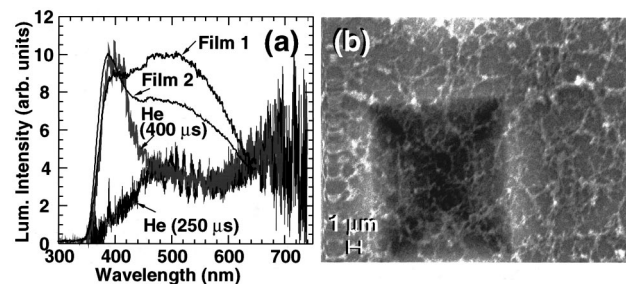


FIG. 3. (a) Comparison of PL spectra (10 nm resolution) from two annealed- SiO_x nanoparticle films and gas-suspended clusters/nanoparticles forming in 10 Torr helium, $d = 2 \text{ cm}$ from the target, at 250 μs (from Fig. 2A) and 400 μs after ablation. Film 1 (prepared in 1 Torr Ar/5% O_2 on cold-finger) and Film 2 (prepared 10 Torr He, RT deposit) were annealed 800 $^\circ\text{C}$ in O_2 (no PL) and then 1000 $^\circ\text{C}$ for 30 min in Ar/5% H_2 gas, giving strong PL at RT under 5.0 eV pulsed excitation. A 320 nm LP filter was used for the films (and He 400 μs) spectra. (b) SEM micrographs of brightly photoluminescent region of annealed Film 1 shows a weblike-aggregate structure which appears to be composed of agglomerated (100–200 nm) network-aggregates of nanoparticles [see Fig. 1(f)].

sub-nm *c*-Si clusters are possible given the TEM measurements, and the stability of the Si–Si vibronic structure with varying particle size and temperatures during the plume expansion indicates that the luminescence likely originates from the surface of the clusters or nanoparticles. For such small Si clusters, contributions from surface atoms may begin to dominate those from the bulk, and the role of surface phonons (~ 53 meV) should also be considered.¹⁹

Pronounced *irregular* structure has been observed on violet and blue-green PL bands from annealed Si-cluster based SRSO films deposited under nonequilibrium processing.^{3–5,13,16,17} Proposed explanations include intrinsic defect centers and quantum-size effects of *c*-Si,²⁰ overlapping cluster emission bands,^{5,21} nanoparticulate SiO₂,³ and Si(II)₀ defects in *a*-SiO₂.^{4,22} Photolysis of surface species¹¹ or the clusters themselves are other possibilities.

However, the most likely explanations for the *regular* vibronic structure of Fig. 2 are photoexcitation of Si–Si vibrations at localized surface states, or from unassigned transitions from highly vibrationally excited Si₂ which is weakly bound or photodissociated from the nanoparticle surface. In support of surface state luminescence, Kimura and Iwasaki reported similar, extremely clear, vibronic structure decorating broad ultraviolet and blue PL bands from isolated (4–10 nm) silicon nanoparticles suspended in organic liquids at room temperature.²³ Unlike the apparent Si–Si vibronic modes in our measurements, Si–O–Si and other modes were found, indicating that the vibronic fine structure originated from a localized surface state.²³ Alternatively, in addition to PL from gas-suspended CdSe nanocrystals, Orii *et al.* also observed strong vibronic luminescence which they attributed to photodissociated Se₂ dimers.²⁴ In both cases, absorption occurs in the bulk of the nanocrystal and luminescence occurs from vibrationally-excited surface states or desorbed species.

Thin films of nanoparticles were collected on Si wafers for comparative PL measurements with our gas-phase results. Imaging revealed that nanoparticles do not readily stick to room temperature (RT) substrates¹⁰ so Si wafers were also mounted onto a cold finger (77 K) which was positioned 4-cm from the *c*-Si target and outside the plume expansion region following KrF laser ablation into flowing gases.

Films collected at RT and 77 K required standard anneals in flowing oxygen at 800 °C and then in Ar/(5% H₂) at 1000 °C before strong RT PL was obtained. As shown in Fig. 3(a), under pulsed UV excitation the broad PL spectra of the annealed films contain violet and green bands in varying proportions which agree in position with those measured at late-times for the gas-suspended nanoparticles. However, this luminescence is fast ($\tau < 10$ ns) and does not exhibit the oscillatory structure observed in Fig. 2. CW excitation of the films at 325 nm revealed 2.1, 2.7, and 3.2 eV bands in order of decreasing intensity.²⁵

In summary, time-resolved photoluminescence from gas-suspended nanoparticles was measured for the first time and correlated with *ex situ* scanning transmission electron microscopy analyses of individual nanoparticles. These techniques provide a mechanism to investigate and modify the optical properties of isolated nanoparticles during synthesis in the gas phase, *prior to deposition*.

Measuring nanoparticles *isolated* in the gas-phase appears to expose luminescence properties *in situ* which are lost, or at least reduced upon deposition. At least for *nc*-Si, while the band gap shifts to the blue with decreasing size, the primary quantum size effect is *isolation* of electron-hole pairs from each other.²⁶ For silicon nanocrystals in thin films, this isolation is provided by an interfacial oxide layer which is crucial to luminescence. The ability to vary the characteristics of this oxide layer as it forms in the gas phase represents a significant processing advantage and may help reveal the origin of visible luminescence in *P*-Si and *nc*-Si.

The authors gratefully acknowledge research assistance by C. W. White and T. Makimura, and valuable discussions with Y. Kanemitsu, K. Kimura, W. Marine, K. Murakami, and K.P. Geohegan. This work was sponsored by the Division of Material Science, U.S. Dept. of Energy under Contract No. DE-AC05-96)R22464 with Lockheed Martin Energy Research Corp.

¹W. L. Wilson, P. F. Szajowski, and L. E. Brus, *Science* **262**, 1242 (1993).

²S. Schuppler, S. L. Friedman, M. A. Marcus, D. L. Adler, Y.-H. Xie, F. M. Ross, Y. J. Chabal, T. D. Harris, L. E. Brus, W. L. Brown, E. E. Chaban, P. F. Szajowski, S. B. Christman, and P. H. Citrin, *Phys. Rev. B* **52**, 4910 (1995).

³L. A. Chiu, A. A. Seraphin, and K. D. Kolenbrander, *J. Electron. Mater.* **23**, 347 (1994).

⁴S. Li, S. J. Silvers, and M. S. El-Shall, *J. Phys. Chem.* **101**, 1794 (1997).

⁵I. A. Movchan, W. Marine, R. W. Dreyfus, H. C. Le, M. Sentis, and M. Autric, *Appl. Surf. Sci.* **96-98**, 251 (1996).

⁶Y. Yamada, T. Orii, I. Umez, S. Takeyama, and T. Yoshida, *Jpn. J. Appl. Phys.*, Part 1 **35**, 1361 (1996).

⁷T. Makimura, Y. Kunii, and K. Murakami, *Jpn. J. Appl. Phys.*, Part 1 **35**, 4780 (1996).

⁸T. Yoshida, Y. Yamada, and T. Orii, *Technical Digest of the International Electron Devices Meeting*, IEEE, San Francisco, CA, Dec. 8-11, 1996, IEEE.

⁹J. Muramoto, Y. Nakata, T. Okada, and M. Maeda, *Jpn. J. Appl. Phys.*, Part 2 **36**, L563 (1997).

¹⁰D. B. Geohegan, A. A. Puzetzy, G. Duscher, and S. J. Pennycook, *Appl. Phys. Lett.* **72**, 2987 (1998).

¹¹Broad reviews have recently been given by P. M. Fauchet, *J. Lumin.* **70**, 294 (1996); F. Koch and V. Petrova-Koch, *J. Non-Cryst. Solids* **198-200**, 846 (1996).

¹²J. P. Proot, C. Delerue, and G. Allan, *Appl. Phys. Lett.* **61**, 1948 (1992); T. Takagahara and K. Takeda, *Phys. Rev. B* **46**, 15578 (1992).

¹³X. Zhao, O. Schoenfeld, S. Komuro, Y. Aoyagi, and T. Sugano, *Phys. Rev. B* **50**, 18654 (1994); *Jpn. J. Appl. Phys.*, Part 2 **33**, L899 (1994).

¹⁴R. E. Hummel, M. H. Ludwig, S. S. Chang, P. M. Fauchet, Ju. V. Vandyshchev, and L. Tsybeskov, *Solid State Commun.* **95**, 553 (1995).

¹⁵H. Morisaki, H. Hashimoto, F. W. Ping, H. Nozawa, and H. Ono, *J. Appl. Phys.* **74**, 2977 (1993).

¹⁶Q. Zhang, S. C. Bayliss, and D. A. Hutt, *Appl. Phys. Lett.* **66**, 1977 (1995).

¹⁷K. Kim, M. S. Suh, T. S. Kim, C. J. Youn, E. K. Suh, Y. J. Shin, K. B. Lee, H. J. Lee, M. H. An, H. J. Lee, and H. Ryu, *Appl. Phys. Lett.* **69**, 3908 (1996).

¹⁸Y. Kanemitsu, N. Shimizu, T. Komoda, P. L. F. Hemment, and B. J. Sealy, *Phys. Rev. B* **54**, R14329 (1996).

¹⁹T. Okada, T. Iwaki, K. Yamamoto, H. Kasahara, and K. Abe, *Solid State Commun.* **49**, 809 (1984).

²⁰L. N. Dinh, L. L. Chase, M. Balooch, W. J. Siekhaus, and F. Wooten, *Phys. Rev. B* **54**, 5029 (1996).

²¹K. D. Rinnen and M. L. Mandich, *Phys. Rev. Lett.* **69**, 1823 (1992).

²²L. N. Skuja, A. N. Streletsky, and A. B. Pakovich, *Solid State Commun.* **50**, 1069 (1984).

²³K. Kimura and S. Iwasaki, *Mater. Res. Soc. Symp. Proc.* **452**, 165 (1997).

²⁴T. Orii, S. Kaito, K. Matsuishi, S. Onari, and T. Arai, *J. Phys.: Condens. Matter* **9**, 4483 (1997).

²⁵Spectrum courtesy T. Makimura (unpublished).

²⁶L. Brus, *J. Phys. Chem.* **98**, 3575 (1994).